Heterologous caffeic acid biosynthesis in *Escherichia coli* is affected by choice of tyrosine ammonia lyase and redox partners for bacterial Cytochrome P450

Kristina Haslinger[1] and Kristala L.J. Prather[1]

[1]Department of Chemical Engineering, Massachusetts Institute of Technology, Cambridge, USA

Correspondence should be directed to kljp@mit.edu

Abstract

Background: Caffeic acid is industrially recognized for its antioxidant activity and therefore its potential to be used as an anti-inflammatory, anticancer, antiviral, antidiabetic and antidepressive agent. It is traditionally isolated from lignified plant material under energy-intensive and harsh chemical extraction conditions. However, over the last decade bottom-up biosynthesis approaches in microbial cell factories have been established, that have the potential to allow for a more tailored and sustainable production. One of these approaches has been implemented in *Escherichia coli* and only requires a two-step conversion of supplemented L-tyrosine by the actions of a tyrosine ammonia lyase and a bacterial Cytochrome P450 monooxygenase. Although the feeding of intermediates demonstrated the great potential of this combination of heterologous enzymes compared to others, no *de novo* synthesis of caffeic acid from glucose has been achieved utilizing the bacterial Cytochrome P450 thus far.

Results: The herein described work aimed at improving the efficiency of this two-step conversion in order to establish de novo caffeic acid formation from glucose. We implemented alternative tyrosine ammonia lyases that were reported to display superior substrate binding affinity and selectivity, and increased the efficiency of the Cytochrome P450 by altering the electron-donating redox system. With this strategy we were able to achieve final titers of more than 300 µM or 47 mg/L caffeic acid over 96 h in an otherwise wild type *E. coli* MG1655(DE3) strain with glucose as the only carbon source. We observed that the choice and gene dose of the redox system strongly influenced the Cytochrome P450 catalysis. In addition, we were successful in applying a tethering

strategy that rendered even an initially unproductive Cytochrome P450/ redox system combination productive.

Conclusions: The caffeic acid titer achieved in this study is about 25% higher than titers reported for other heterologous caffeic acid pathways in wildtype *E. coli* without L-tyrosine supplementation. The tethering strategy applied to the Cytochrome P450 appears to be particularly useful for non-natural Cytochrome P450/redox partner combinations and could be useful for other recombinant pathways utilizing bacterial Cytochromes P450.

Keywords

Caffeic acid, Cytochrome P450, tethering, PUPPET, recombinant pathway

Background

Caffeic acid is widely recognized for its medicinal potential due to its antidepressive [1], antihyperglycemic [2], anti-inflammatory [3], antioxidant [2, 4], anti-coagulatory [3], anticancer [5] and antiviral [6] properties. It is readily produced in plants as a key intermediate in phenylpropanoid biosynthesis. In this pathway, phenylalanine is diverted from primary metabolism by a phenylalanine ammonia lyase associated with the endoplasmatic reticulum and transformed into *trans*-cinnamic acid. Cinnamic acid is then hydroxylated by the membrane-anchored Cytochrome P450 enzymes cinnamate 4-hydroxylase (C4H) and *p*-coumarate 3-hydroxylase to *p*-coumarate and caffeic acid, respectively [7, 8]. From there a range of molecules can be produced that serve as lignin building blocks or precursors for secondary metabolites such as tannins, (iso)flavonoids, anthocyanins, stilbenes and coumarins [9]. All of these compounds have high market value but are difficult to isolate because they are of low natural

abundance (e.g. stilbenes and coumarins), or challenging to extract (e.g. lignin-derived aromatics) [10]. Therefore, over the last decade various strategies have been developed to implement biosynthetic pathways in microbial cell factories that promise their tailored biosynthesis in a sustainable manner. Recent examples are the production of stilbenoids and flavonoids in *Corynebacterium glutamicum* [11, 12], and curcumin [13, 14] and caffeic acid [14–24] in *Escherichia coli*. For the biosynthesis of *p*-coumaric acid in *E. coli*, it was found that using L-tyrosine as a pathway precursor was superior over phenylalanine [25], since activity of the plant Cytochrome P450 enzyme C4H could not be reconstituted as of recently [26]. Based on this finding, two major strategies have been devised to produce caffeic acid that employ microbial tyrosine ammonia lyases (TAL) to generate *p*-coumaric acid followed by either (1) a flavin-dependent HpaBC-type oxidoreductase complex (4-hydroxyphenylacetate 3-hydroxylase, PFAM PF03241) from *Saccharothrix espanaensis* [14–18], *E. coli* [19–21], *Thermus thermophilus* HB8 [20] or *Pseudomonas aeruginosa* [22, 23], or (2) a bacterial cytochrome P450 enzyme CYP199A2 F185L from *Rhodopseudomonas palustris* [14, 18, 24]. In all of these studies it became evident that the caffeic titers are rather low unless L-tyrosine or *p*-coumaric acid are added to the growth media, or the aromatic amino acid pathway is engineered to increase intracellular L-tyrosine levels. For the pathways utilizing HpaBC-type oxidoreductases, the highest titer reported for *de novo* synthesis in wild-type *E. coli* to date is 42 mg/L (*S. espanaensis* TAL and HpaBC) [17]. However, to our knowledge no *de novo* synthesis has been reported for pathways utilizing CYP199A2 F185L.

In this study, we established *de novo* biosynthesis of caffeic acid from glucose through the actions of TAL and CYP199A2 F185L NΔ7. In order to achieve this goal, we tested

TALs from three different organisms and explored strategies to enhance the activity of CYP199A2 F185L NΔ7. We found that driving the binding equilibrium of the electron-donating redox partners to CYP199A2 F185L NΔ7 towards the bound state improves pathway titers and enabled us to produce ~47 mg/L caffeic acid from glucose in wildtype *E. coli* MG1655(DE3). This titer is slightly higher than the titers reported for the HpaBC-based pathways in wildtype *E. coli* with glucose as the only carbon source [17, 19].

Results

In an earlier study Rodrigues et al. demonstrated the two-step conversion of 3 mM L-tyrosine to caffeic acid in *E. coli* MG1655(DE3) expressing the enzymes RgTAL and CYP199A2 F185L NΔ7 with redox partners, without reporting *de novo* production of caffeic acid from glucose (Figure 1) [18]. In this study we set out to improve these enzymatic steps to establish caffeic acid production from glucose without supplementing L-tyrosine. When examining the two-step conversion more closely, we determined that both pathway steps needed improvement. First, the efficiency of the committed step, the conversion of L-tyrosine to *p*-coumaric acid, determines how much L-tyrosine is withdrawn from primary metabolism and fed into the pathway. Therefore, we hypothesized that TAL variants with higher selectivity and affinity for L-tyrosine would improve pathway flux. Second, the hydroxylation of *p*-coumaric acid to caffeic acid catalyzed by CYP199A2 F185L NΔ7 appears to be a bottleneck in the pathway, since *p*-coumaric acid accumulates in the fermentation [18]. This accumulation is thought to be detrimental because *p*-coumaric acid has been shown to inhibit TAL activity and to be cytotoxic [27, 28]. Since a common problem with Cytochrome P450 catalyzed reactions is the protein-protein interaction with redox partners, which is strictly required for

electron transfer and substrate turnover [29], we hypothesized that driving the assembly of the redox complex would lead to higher product titers.

To improve the first pathway step, we selected two homologous tyrosine ammonia lyases with supposedly superior characteristics compared to RgTAL, namely a stronger selectivity for L-tyrosine over L-phenylalanine, higher substrate affinity (K_m) and superior catalytic efficiency (k_{cat}/K_m) (Supporting Information Table S1) [30]. We chose FjTAL from *Flavobacterium johnsoniae* and SeSam8 from *Saccharothrix espanaensis* and obtained the synthetic genes codon-optimized for expression in *E. coli*. In a first pass, utilizing these two TALs in the same three plasmid expression system as used by Rodrigues et al., and providing glucose as the only carbon source, we observed accumulation of caffeic acid 72 h post induction (p. i.). The highest titers of caffeic acid and *p*-coumaric acid are seen with the FjTAL enzyme (Figure 2A, strain s02). In a parallel experiment, where 3 mM L-tyrosine was fed in addition to glucose, the final caffeic acid titers were comparable among the three strains (Figure 2B). This indicates that all enzymes are able to efficiently route L-tyrosine into the caffeic acid pathway at high L-tyrosine concentrations, whereas FjTAL outperforms the other enzymes under low L-tyrosine conditions and is therefore a strong candidate for this pathway.

Next, we sought to improve the efficiency of the second pathway step, the hydroxylation of *p*-coumaric acid to caffeic acid catalyzed by CYP199A2 F185L NΔ7, by enhancing the efficiency of the electron transfer step from the two redox partner proteins to CYP199A2 F185L NΔ7. To achieve this goal, we tested three strategies: 1. the use of alternative redox partners, 2. the tethering of the redox complex by creating genetic fusions with high-affinity tethering domains, and 3. the supply of extra gene copies

coding for one of the redox partners. To facilitate cloning from here on in the study, we use both multiple cloning sites of the pETDuet vector for the genes encoding redox enzymes rather than the bicistronic pKVS45 vector (see Tables 1 and 2).

For class I Cytochromes P450, two redox partners are required to provide two electrons from NAD(P)H: an iron-sulfur cluster containing ferredoxin (Fdx) and a flavin-dependent ferredoxin reductase (FdR) [31]. Rodrigues et al. utilized a redox system composed of palustrisredoxin (Pux) and putidaredoxin reductase (PdR), which had been used in the original characterization of CYP199A2 [32]. This is, however, not the natural redox system for CYP199A2, since the palustrisredoxin reductase PuR was only identified and characterized a few years later [33]. Although the Pux/PdR redox system has been proven to support substrate turnover, it remained unclear whether the assembly of the trimeric complex and the respective redox potentials of the proteins supported optimal electron transfer. Therefore, we decided to test the natural redox system (Pux/PuR) alongside a well-characterized surrogate redox system (Pdx/PdR). We determined the caffeic acid titers 72 h p. i. with supplementation of *p*-coumaric acid for three strains expressing CYP199A2 F185L NΔ7 and one of the three respective redox systems Pux/PdR (hybrid, s04), Pux/PuR (natural, s05), Pdx/PdR (surrogate, s06). We observed the highest titers for the natural redox system (s05) and no turnover with the full surrogate system composed of Pdx/PdR (Figure 3A). This suggests that the electron transfer from ferredoxin to CYP199A2 F185L NΔ7 is severely impaired with the surrogate ferredoxin Pdx, whereas the electron transfer from PdR to Pux in the hybrid system appears to sufficiently support substrate turnover. The native redox complex Pux/PuR, however, displays the highest catalytic power and a titer of 1.6 +/- 0.32 mM

caffeic acid was observed which corresponds to 53% conversion of the fed *p*-coumaric acid. These results indicate that the careful choice of redox system is crucial for this pathway step.

With our second strategy, we sought to further improve these redox systems by generating genetic fusions of the enzymes with the subunits of the heterotrimeric DNA sliding clamp PCNA (Proliferating Cell Nuclear Antigen) of *Sulfolobus solfataricus* P2 [34]. This PCNA complex has been shown to tolerate the fusion of other genes to the ‘3 ends (C-termini) [35] of its three subunits, while maintaining their high binding affinity towards each other: the PCNA1/PCNA2 dimer has a dissociation constant in the low picomolar range and the PCNA1/PCNA2/PCNA3 trimer in the high nanomolar range [34]. This fusion strategy has been shown to be highly efficient for the *in vitro* reconstitution of Cytochrome P450 activity and was termed PUPPET by the inventors (PCNA-utilized protein complex of P450 and its two electron transfer-related proteins) [35–40]. To our knowledge, this strategy hasn’t been used in whole-cell catalysis to date. Initially, we tested fusion proteins analogous to the previously described PUPPET fusions with FdR fused to the C-terminus of PCNA domain 1, Fdx to PCNA2 and the Cytochrome P450 to PCNA3 (tether design I, strains s07-s09; Figure 3B). When feeding 3 mM *p*-coumaric acid, we observed higher titers of caffeic acid for all tethered redox systems than compared to the respective free enzymes. The effect was more pronounced with the hybrid and surrogate systems, where a 6-fold increase in titer was observed for Pux/PdR (s07) and an 8-fold increase for Pdx/PdR (s09). Overall, the highest titer was observed with the tethered version of Pux/PdR (s07, titer: 2.3 +/- 0.07 mM). Next, we investigated whether these titers could be further improved by

generating a new arrangement of the fusion partners. Based on the published dissociation constants for the well-studied Cytochrome P450 CYP101A1 and its redox partners [41, 42], we assumed that the affinity of Fdx to FdR is about 100-fold higher than the affinity of Fdx to the Cytochrome P450. We hypothesized that the high affinity interaction between PCNA1 and PCNA2 might be even more beneficial to the low affinity interaction between the Cytochrome P450 and Fdx than between Fdx and FdR. Therefore, we generated a second set of fusion genes (tether design II), where CYP199A2 F185L NΔ7 is fused to PCNA1, Fdx to PCNA2 and FdR to PCNA3, while maintaining the linker arrangements that had previously been optimized for the respective elements of the redox complex [39] (s 10-s12, Fig 3C). With these alternative tethering constructs, the highest final caffeic acid titers were obtained with the surrogate Pdx/PdR redox system (s10, titer: 2.1 +/- 0.35 mM), while the titers obtained with the other redox systems were lower than in the previous experiments. This indicates that the domain arrangements in the second tether design supports the weaker protein-protein interactions in the surrogate redox complex better than the other tether design, whereas it disturbs catalysis with the two redox systems that already led to high titers with free redox partners and tether design I.

Next, we tested the best redox partner constructs in the context of the full pathway with FjTAL as the first pathway enzyme (Figure 3D). We observed the highest caffeic acid titers with the untethered, natural redox partners (Pux/PuR, s15, titer: 0.14 +/- 0.028 mM). Although strains s07, s08 and s12 had slightly outperformed s05 in the one-step conversion, the corresponding strains expressing FjTAL (s14, s16, s17, respectively) yielded lower caffeic acid titers in the two-step recombinant pathway. The

cost for expressing the additional tethering domains may offset the positive effects of the enhanced enzymatic activity. In all of the fermentations, lower final titers of *p*-coumaric acid are measured than in the initial test of FjTAL (s02), which indicates that the changes made to the second pathway step allow for an almost complete conversion to the final product.

Lastly, we tested whether additional copies of the palustrisredoxin encoding gene, *pux*, would further improve the performance of the so far best pathway configuration with FjTAL and the natural redox partners of CYP199A2 F185L NΔ7 (Pux/PuR redox system). Therefore, we inserted *pux* into MCS1 of plasmid IR64 pCDFDuet::_6His-CYP199A2 F185L NΔ7, yielding plasmid c84 pCDFDuet::6His-Pux_6His-CYP199A2F185L NΔ7. Based on the supplier's reports (Novagen), the copy numbers of pETDuet and pCDFDuet are in a similar range so that the incorporation of an additional gene copy into pCDFDuet should lead to an estimated doubling of the gene dose and potentially the level of protein expressed. When comparing the strain harboring this set of plasmids (s18) to the RgTAL control strain (s13) and the strain expressing FjTAL and Pux/PuR (s15), we observed an increase in caffeic acid titer with full consumption of the intermediate *p*-coumaric acid (Figure 4A). This indicates that the availability of Pux was previously insufficient and that a higher expression level of this protein supports better Cytochrome P450 performance. Despite the improvements in final caffeic acid titer, we observed an accumulation of *p*-coumaric acid in early fermentation until 48 h p. i. and then a sharp drop in titer until it is fully converted to caffeic acid at 96 h p. i. (Figure 4B). This indicates that in early fermentation the first pathway step is still faster than the second pathway step. In late fermentation, the conversion of *p*-coumaric acid to caffeic

acid is faster than the formation of the intermediate, or no additional *p*-coumaric acid is formed. This could be caused by the lack of available L-tyrosine once the cultures reach stationary phase, although we did not observe increased titers when spiking the cultures with 3 mM L-tyrosine at 48 h p. i. (I Figure S1). Therefore, we are inclined to suggest that the tyrosine ammonia lyase has lost its activity by that time. Potential causes could be structural instability of the TAL enzyme or its inhibition by the intermediate as described previously [27]. Overall, with the exchange of RgTAL for FjTAL and the change of the redox system from Pux/PdR to Pux/PuR with an additional gene copy of *pux*, we improved this recombinant pathway and were able to produce caffeic acid from glucose without feeding L-tyrosine. The highest final titer after 96 h of fermentation was 47 mg/L, which is slightly higher than caffeic acid titers achieved with other recombinant pathways without L-tyrosine supplementation [17, 19]. Furthermore, the improved pathway is able to convert >50% of fed L-tyrosine to caffeic acid (SI Figure S1), which indicates that it should be able to produce high amounts of caffeic acid in a tyrosine-producer strain.

Discussion

Building microbial cell factories for the production of plant polyphenols has been a major goal for metabolic engineers over the last decade [43, 44]. The low abundance of these compounds and their occurrence in complex mixtures of variable composition in plants, makes recombinant microbial cell factories an attractive source for industrial applications. However, the strict regulation of the aromatic amino acid metabolism, which provides precursors to most recombinant polyphenol-producing pathways, limits the overall pathway efficiency. For recombinant polyphenol-producing pathways in

E.coli, it has been observed that overcoming the precursor bottleneck by metabolic engineering of the aromatic amino acid pathway, often reveals bottlenecks further down the recombinant pathway [45–47]. Therefore, it is crucial to optimize the recombinant pathway itself before moving into a microbial chassis with deregulated aromatic amino acid production. In this study, we optimized the two-step conversion of L-tyrosine to caffeic acid. Here it is important to ensure high efficiency of the second pathway step to avoid accumulation of *p*-coumaric acid, which has been shown to severely inhibit the activity of the first pathway enzyme, TAL [27]. The three strategies we tested focused on the electron-donating redox partners rather than the Cytochrome P450 enzyme itself. Previous *in vitro* studies of this particular Cytochrome P450 and others have shown that the right choice of redox system, in particular the ferredoxin, is crucial for efficient electron transfer and enzyme catalysis [29, 33]. As expected, we observed the highest caffeic acid titers with the natural redox system composed of Pux and PuR in the one-step conversion with untethered redox partners. However, when we applied tethering strategies to increase the affinity of the Cytochrome P450 and the redox partners towards each other, we observed higher titers with the non-natural redox partners. Tethering strategies have previously been applied to several Cytochrome P450 enzymes, both *in vitro* [35, 42, 48–51] and *in vivo* [42, 48]. The *in vitro* studies showed that tethered redox complexes are able to overcome the need to use an excess of redox partners over the Cytochrome P450 enzyme, to compensate for low protein-protein affinities (typically a five- to twenty-fold molar excess of ferredoxin is used *in vitro*). Furthermore, kinetic studies showed that at low enzyme concentrations, the tethered complexes outperform the 1:1:1 mixtures of free enzymes. These reports and our

findings for our versions of the PUPPET tether indicate that tethering strategies in whole-cell catalysis may be particularly useful in two scenarios: (A) if the expression levels of the Cytochrome P450 and redox partners are low (poor protein expression, expression from genomic gene copies or as part of a multi-enzyme recombinant pathway), or (B) if the natural redox partners are unknown and surrogate systems are used to reconstitute the Cytochrome P450 activity.

To our knowledge, this study is the first one to use the PUPPET tether in whole-cell catalysis and also the first one to use any of the known Cytochrome P450 tethers in the context of a recombinant pathway. In the caffeic acid pathway, the tethered Cytochrome P450 complexes were slightly outperformed by the free, natural redox complex, in particular in the presence of extra copies of the *pux* gene (s18). This may indicate that the metabolic burden of expressing the PCNA subunits in addition to the pathway enzymes and the three resistance genes required for plasmid maintenance represents a disadvantage of the strains expressing the tethered Cytochrome P450 complexes compared to the ones expressing the free, natural redox complex (s15 and s18). The fact that s18 outperforms s15 indicates that the availability of Pux is limiting in s15, and is in good agreement with observations made in other whole-cell conversions [52, 53]. Since our strategy only doubled the gene dose of *pux*, it is very well possible that rearranging the genes in the vector system to achieve higher protein levels of Pux relative to the other enzymes could lead to even better results than described in this study. Our optimization efforts of the second pathway step in combination with the use of FjTAL for the first pathway step, enabled us to demonstrate the *de novo* production of caffeic acid in an otherwise wild type *E. coli* background. FjTAL had previously been

seen to be beneficial for the production of *p*-coumaric acid and its derivatives in other microbes [11, 54, 55], however, to our knowledge it has not been used in *E. coli*. It appears that this enzyme allows for a more efficient routing of L-tyrosine into the caffeic acid pathway than RgTAL at low L-tyrosine concentrations. Under high L-tyrosine conditions, at levels that we would expect in tyrosine producer strains [56], our fermentation strains expressing FjTAL achieve slightly higher caffeic acid titers than the strains expressing RgTAL and lower titers of *p*-coumaric acid. This indicates that the optimized pathway is more balanced so that less *p*-coumaric acid accumulates but overall less L-tyrosine is converted into *p*-coumaric acid. To further improve these results, it is necessary to investigate the stability and activity of the FjTAL enzyme over time, since it appears to be inactive after 48h of fermentation.

Conclusions

In this study we established *de novo* synthesis of caffeic acid by expressing tyrosine ammonia lyase from *Flavobacterium johnsoniae* and CYP199A2 F185L N□7 from *Rhodopseudomonas palustris* with its redox partners palustrisredoxin and palustrisredoxin reductase. We found that compared to earlier versions of this pathway, changes made to the redox partners, namely the use of palustrisredoxin reductase instead of putidaredoxin reductase and the duplication of the palustrisredoxin gene dose, as well as the use of FjTAL instead of RgTAL, enhanced the pathway performance under low L-tyrosine conditions as encountered in otherwise wild type *E. coli*. Furthermore, we observed that applying a tethering strategy to the Cytochrome P450-catalyzed pathway step based on the PUPPET system [35] increases caffeic acid titers in strains expressing non-natural redox systems. This indicates that this strategy

309 can be useful for pathways containing orphan bacterial Cytochromes P450. The
310 optimized caffeic acid pathway could now be transferred into a tyrosine-producer *E. coli*
311 strain for more in-depth characterization or process engineering.

312 Materials and Methods

313 Bacterial strains and plasmids

314 All molecular cloning and plasmid propagation steps were performed in chemically
315 competent *Escherichia coli E. cloni*® 10G (F- *mcrA* Δ(*mrr-hsd*RMS-
316 *mcr*BC) *end*A1 *rec*A1 Φ80*dlac*ZΔM15 Δ*lac*X74 *ara*D139
317 Δ(*ara,leu*)7697*gal*U *gal*K *rps*L *nup*G λ- *ton*A) produced by Lucigen (Middleton, WI,
318 USA). Gene expression under the control of T7 promoters was performed in *E. coli* K-12
319 MG1655(DE3) [57]. Plasmids were constructed with a range of strategies summarized
320 in the Supplementary Information (SI) Table S2. All genes in the final constructs were
321 fully sequenced (Eton Bioscience, Charlestown, MA). The FjTAL, SeSam8 and PCNA1-
322 PdR genes were codon optimized for *E. coli* and synthesized as gblocks® gene
323 fragments by Integrated DNA Technologies (Coralville, IA, USA) (sequence provided in
324 SI). Plasmids pHSG-PCNA2 and pHSG-PCNA3 were a gift from Teruyuki Nagamune
325 obtained through Addgene (Cambridge, MA, USA) (Addgene plasmid # 66126;
326 http://n2t.net/addgene:66126; RRID:Addgene_66126) and (Addgene plasmid # 66127;
327 http://n2t.net/addgene:66127; RRID:Addgene_66127) [35]. Plasmid pACYCDuet-
328 PuR/Pux was a gift from Dr. Stephen G. Bell (University of Adelaide, Australia). The
329 construction of plasmids IR54 and IR64 is described in Rodrigues et al 2015 [18].
330 The peptide linkers connecting the PCNA subunits with the respective enzymes were
331 designed based on the optimized linkers described in Haga et al. 2013 [39] (tether

design I: PCNA1-$(GGGS)_2$-FdR, PCNA2-$GGGSP_{20}$G-Fdx, PCNA3-GGS-Cytochrome P450; tether design II: PCNA1-GGS-Cytochrome P450, PCNA2-$GGGSP_{20}$G-Fdx, PCNA3-$(GGGS)_2$-FdR).

Fermentation

Plasmids and strains used in fermentations are described in Table 1 and Table 2, respectively. *E. coli* K-12 MG1655(DE3) made chemically competent according to the protocol by Inoue et al [58] was sequentially transformed with appropriate plasmids. The correct identity of strains was confirmed by colony PCR. Starter cultures were prepared from three individual colonies of the final strains in 5 mL Lysogeny broth (LB) supplemented with carbenicillin (100 µg/mL), spectinomycin (50 µg/mL) and kanamycin (50 µg/mL, only s01-s03 and s13-s18) in round-bottom polystyrene tubes, incubated over night at 37°C with agitation and used to inoculate the main cultures (7 mL LB with antibiotics; round-bottom polystyrene tubes). After 4 h of growth at 37°C, 250 rpm, OD_{600} was measured and the appropriate volume of each culture pelleted and resuspended in modified, selective M9 including substrates and 4% glucose to obtain 15 mL cultures at OD_{600} of 0.7 or 20 mL cultures at OD_{600} of 0.5 to 0.7 (time course experiment) in sterile glass tubes. These cultures were incubated at 26°C, 160 rpm for 72 h or 96 h (time course experiment). For the time course experiment samples of 1000 µL were taken every 24 h, for all other experiments samples of 2000 µL were taken after 72 h and either stored at -20°C until further processing or extracted with ethyl acetate immediately.

M9 medium composition (1x) prepared from sterile stocks: M9 salts (Millipore-Sigma, used as 5x stock), Trace Mineral Supplement (ATCC® MD-TMS™, used as 200x stock), vitamin mix (from 100x stock; final: riboflavin 0.84 mg/L, folic acid 0.084 mg/L,

nicotinic acid 12.2 mg/L, pyridoxine 2.8 mg/L, and pantothenic acid 10.8 mg/L), biotin (from 1000x stock; final: 0.24 mg/L), thiamine (from 1470x stock; final: 340 mg/L), δ-Aminolevulinic acid (from 1000x stock in MeOH, final: 7.5 µg/mL), IPTG (from 1000x stock, final: 1 mM), aTc (from 1000x stock, final: 100 ng/mL; only included in fermentations of s01-s03), carbenicillin (from 1000x stock, final: 100 µg/mL), spectinomycin (from 1000x stock, final: 50 µg/mL), kanamycin (from 1000x stock, final: 50 µg/mL, only strains s01-s03 and s13-s18), 4% (w/v) glucose (from 50% w/v stock). Optional: *p*-coumaric acid (from fresh 100x stock in MeOH, final 3 mM) or L-tyrosine (from fresh 100x stock in 1M HCl).

Product extraction

The samples were acidified with 6N HCl (pH<3) and split into two tubes as technical duplicates. Samples were extracted twice with equal volumes of ethylacetate. The organic phases of both extraction steps were combined and evaporated under a stream of air or nitrogen. The dried material was resuspended in 100 µL Acetonitrile with 0.1% Trifluoracetic acid (10x concentrated compared to culture) or 80 µL Acetonitrile with 0.1% Trifluoracetic acid (5x concentrated compared to culture) for the time course experiment. Samples were transferred into HPLC vials with conical glass inserts and analyzed by HPLC.

HLPC analysis

10 µL of the samples were analyzed by reversed-phase HPLC (instrument: Agilent 1100, column: Agilent Zorbax Eclipse XDB-C18 80Å, 4.6 x 150 mm, 5µm; detector: Agilent diode array detector G1315B, λ=310nm, gradient: 10% to 20% Acetonitrile with 0.1% Trifluoracetic acid over 17 min. The *p*-coumaric acid and caffeic acid peaks were identified by comparing the retention times to authentic standards and by mass

spectrometry (Agilent G6120, quadrupole MS). The integrated peak areas were converted to concentrations in mM based on calibration curves generated with authentic standards.

List of abbreviations

FdR – ferredoxin reductase

Fdx – ferredoxin

FjTAL – *F. johnsoniae* tyrosine ammonia lyase

PdR – *P. putida* putidaredoxin reductase

Pdx – *P. putida* putidaredoxin

PCNA - Proliferating Cell Nuclear Antigen = heterotrimeric DNA sliding clamp; used as tether

p. i. – post induction

PuR – *R. palustris* palustrisredoxin reductase

Pux – *R. palustris* palustrisredoxin

RgTAL – *R. glutinis* tyrosine ammonia lyase

TAL – tyrosine ammonia lyase

Declarations

Ethics approval and consent to participate

Not applicable.

Consent for publication

Not applicable.

Availability of data and materials

The datasets used and/or analyzed during the current study are available from the corresponding author on reasonable request.

Competing interests

The authors declare that they have no competing interests.

Funding

K.H. is supported by the Human Frontier Science Program (Grant Number LT000969/2016-L). Research was supported by the MIT Portugal Program (Grant Number 6937822).

Authors' contributions

K.H. conceived the study and wrote the manuscript with support and guidance by K.L.J.P. K.H. performed and analyzed the experiments.

Acknowledgements

K.H. and K.L.J.P. are grateful to Dr. Stephen G. Bell (University of Adelaide, Australia) for plasmid pACYCDuet::PuR_Pux, and David Poberejsky for assistance with cloning. K.H. is grateful for the support by the Human Frontier Science Program (Grant Number LT000969/2016-L). This work was supported by the MIT Portugal Program (Grant Number 6937822).

References

1. Takeda H, Tsuji M, Inazu M, Egashira T, Matsumiya T. Rosmarinic acid and caffeic acid produce antidepressive-like effect in the forced swimming test in mice. European Journal of Pharmacology. 2002;449:261–7. doi:10.1016/S0014-2999(02)02037-X.

2. Jung UJ, Lee M-K, Park YB, Jeon S-M, Choi M-S. Antihyperglycemic and antioxidant

424 properties of caffeic acid in db/db mice. The Journal of pharmacology and experimental
425 therapeutics. 2006;318:476–83. doi:10.1124/jpet.106.105163.

426 3. Chao P-C, Hsu C-C, Yin M-C. Anti-inflammatory and anti-coagulatory activities of
427 caffeic acid and ellagic acid in cardiac tissue of diabetic mice. Nutrition & metabolism.
428 2009;6:33. doi:10.1186/1743-7075-6-33.

429 4. Mori H, Iwahashi H. Antioxidant Activity of Caffeic Acid through a Novel Mechanism
430 under UVA Irradiation. Journal of Clinical Biochemistry and Nutrition. 2009;45:49–55.

431 5. Rajendra Prasad N, Karthikeyan A, Karthikeyan S, Venkata Reddy B. Inhibitory effect
432 of caffeic acid on cancer cell proliferation by oxidative mechanism in human HT-1080
433 fibrosarcoma cell line. Molecular and Cellular Biochemistry. 2011;349:11–9.
434 doi:10.1007/s11010-010-0655-7.

435 6. Yamasaki H, Tsujimoto K, Uozaki M, Nishide M, Suzuki Y, Koyama AH, et al.
436 Inhibition of multiplication of herpes simplex virus by caffeic acid. International Journal
437 of Molecular Medicine. 2011;28:595–8. doi:10.3892/ijmm.2011.739.

438 7. Rasmussen S, Dixon RA. Transgene-Mediated and Elicitor-Induced Perturbation of
439 Metabolic Channeling at the Entry Point into the Phenylpropanoid Pathway. The Plant
440 Cell. 1999;11:1537–52. doi:10.1105/tpc.11.8.1537.

441 8. Achnine L, Blancaflor EB, Rasmussen S, Dixon RA. Colocalization of L-
442 Phenylalanine Ammonia-Lyase and Cinnamate 4-Hydroxylase for Metabolic Channeling
443 in Phenylpropanoid Biosynthesis. The Plant cell. 2004;16:3098–109.
444 doi:10.1105/tpc.104.024406.

445 9. Vogt T. Phenylpropanoid biosynthesis. Molecular Plant. 2010;3:2–20.
446 doi:10.1093/mp/ssp106.

447 10. Wendisch VF, Kim Y, Lee J-H. Chemicals from lignin: Recent depolymerization
448 techniques and upgrading extended pathways. Current Opinion in Green and
449 Sustainable Chemistry. 2018;14:33–9. doi:10.1016/J.COGSC.2018.05.006.

450 11. Kallscheuer N, Vogt M, Stenzel A, Gätgens J, Bott M, Marienhagen J. Construction
451 of a *Corynebacterium glutamicum* platform strain for the production of stilbenes and
452 (2S)-flavanones. Metabolic Engineering. 2016;38:47–55.
453 doi:10.1016/j.ymben.2016.06.003.

454 12. Kallscheuer N, Vogt M, Bott M, Marienhagen J. Functional expression of plant-
455 derived O-methyltransferase, flavanone 3-hydroxylase, and flavonol synthase in
456 *Corynebacterium glutamicum* for production of pterostilbene, kaempferol, and quercetin.
457 Journal of Biotechnology. 2017;:1–7. doi:10.1016/j.jbiotec.2017.01.006.

458 13. Rodrigues JL, Araújo RG, Prather KLJ, Kluskens LD, Rodrigues LR. Production of
459 curcuminoids from tyrosine by a metabolically engineered *Escherichia coli* using caffeic
460 acid as an intermediate. Biotechnology Journal. 2015;10:599ß609.
461 doi:10.1002/biot.201400637.

462 14. Rodrigues JL, Couto MR, Araújo RG, Prather KLJ, Kluskens L, Rodrigues LR.
463 Hydroxycinnamic acids and curcumin production in engineered *Escherichia coli* using
464 heat shock promoters. Biochemical Engineering Journal. 2017;125:41–9.
465 doi:10.1016/J.BEJ.2017.05.015.

466 15. Choi O, Wu C-Z, Kang SY, Ahn JS, Uhm T-B, Hong Y-S. Biosynthesis of plant-

467 specific phenylpropanoids by construction of an artificial biosynthetic pathway in
468 *Escherichia coli*. Journal of Industrial Microbiology & Biotechnology. 2011;38:1657–65.
469 doi:10.1007/s10295-011-0954-3.

470 16. Zhang H, Pereira B, Li Z, Stephanopoulos G. Engineering *Escherichia coli* coculture
471 systems for the production of biochemical products. Proceedings of the National
472 Academy of Sciences of the United States of America. 2015;112:8266–71.
473 doi:10.1073/pnas.1506781112.

474 17. Kang S-Y, Choi O, Lee JK, Hwang BY, Uhm T-B, Hong Y-S. Artificial biosynthesis of
475 phenylpropanoic acids in a tyrosine overproducing *Escherichia coli* strain. Microbial Cell
476 Factories. 2012;11:1–9. doi:10.1186/1475-2859-11-153.

477 18. Rodrigues JL, Araújo RG, Prather KLJ, Kluskens LD, Rodrigues LR. Heterologous
478 production of caffeic acid from tyrosine in *Escherichia coli*. Enzyme and Microbial
479 Technology. 2015;71:36–44. doi:10.1016/j.enzmictec.2015.01.001.

480 19. Lin Y, Yan Y. Biosynthesis of caffeic acid in *Escherichia coli* using its endogenous
481 hydroxylase complex. Microbial Cell Factories. 2012;11:42. doi:10.1186/1475-2859-11-
482 42.

483 20. Huang Q, Lin Y, Yan Y. Caffeic acid production enhancement by engineering a
484 phenylalanine over-producing *Escherichia coli* strain. Biotechnology and
485 Bioengineering. 2013;110:3188–96. doi:10.1002/bit.24988.

486 21. Wang J, Mahajani M, Jackson SL, Yang Y, Chen M, Ferreira EM, et al. Engineering
487 a bacterial platform for total biosynthesis of caffeic acid derived phenethyl esters and
488 amides. Metabolic Engineering. 2017;44 September:89–99.

489 doi:10.1016/j.ymben.2017.09.011.

490 22. Furuya T, Kino K. Catalytic activity of the two-component flavin-dependent
491 monooxygenase from *Pseudomonas aeruginosa* toward cinnamic acid derivatives.
492 Applied Microbiology and Biotechnology. 2014;98:1145–54.

493 23. Kawaguchi H, Katsuyama Y, Danyao D, Kahar P, Nakamura-Tsuruta S, Teramura
494 H, et al. Caffeic acid production by simultaneous saccharification and fermentation of
495 kraft pulp using recombinant *Escherichia coli*. Applied Microbiology and Biotechnology.
496 2017;101:5279–90. doi:10.1007/s00253-017-8270-0.

497 24. Furuya T, Arai Y, Kino K. Biotechnological production of caffeic acid by bacterial
498 cytochrome P450 CYP199A2. Applied and Environmental Microbiology. 2012;78:6087–
499 94.

500 25. Watts KT, Lee PC, Schmidt-Dannert C. Exploring Recombinant Flavonoid
501 Biosynthesis in Metabolically Engineered *Escherichia coli*. ChemBioChem. 2004;5:500–
502 7. doi:10.1002/cbic.200300783.

503 26. Li Y, Li J, Qian B, Cheng L, Xu S, Wang R. De Novo Biosynthesis of p-Coumaric
504 Acid in *E. coli* with a trans-Cinnamic Acid 4-Hydroxylase from the Amaryllidaceae Plant
505 *Lycoris aurea*. Molecules. 2018;23:3185.

506 27. Sariaslani FS. Development of a combined biological and chemical process for
507 production of industrial aromatics from renewable resources. Annual review of
508 microbiology. 2007;61:51–69.

509 28. Xue Z, McCluskey M, Cantera K, Ben-Bassat A, Sariaslani FS, Huang L. Improved

510 production of p-hydroxycinnamic acid from tyrosine using a novel thermostable
511 phenylalanine/tyrosine ammonia lyase enzyme. Enzyme and Microbial Technology.
512 2007;42:58–64.

513 29. Bell SG, McMillan JHC, Yorke J a., Kavanagh E, Johnson EOD, Wong L-L. Tailoring
514 an alien ferredoxin to support native-like P450 monooxygenase activity. Chemical
515 Communications. 2012;:11692–4.

516 30. Jendresen CB, Stahlhut SG, Li M, Gaspar P, Siedler S, Förster J, et al. Novel highly
517 active and specific tyrosine ammonia-lyases from diverse origins enable enhanced
518 production of aromatic compounds in bacteria and yeast. Applied and Environmental
519 Microbiology. 2015; April. doi:10.1128/AEM.00405-15.

520 31. Hannemann F, Bichet A, Ewen KM, Bernhardt R. Cytochrome P450 systems--
521 biological variations of electron transport chains. Biochim Biophys Acta.
522 2007;1770:330–44. doi:10.1016/j.bbagen.2006.07.017.

523 32. Bell SG, Hoskins N, Xu F, Caprotti D, Rao Z, Wong L-L. Cytochrome P450 enzymes
524 from the metabolically diverse bacterium *Rhodopseudomonas palustris*. Biochemical
525 and Biophysical Research Communications. 2006;342:191–6.

526 33. Xu F, Bell SG, Peng Y, Johnson EOD, Bartlam M, Rao Z, et al. Crystal structure of a
527 ferredoxin reductase for the CYP199A2 system from *Rhodopseudomonas palustris*.
528 Proteins. 2009;77:867–80. doi:10.1002/prot.22510.

529 34. Dionne I, Nookala RK, Jackson SP, Doherty AJ, Bell SD. A heterotrimeric PCNA in
530 the hyperthermophilic archaeon Sulfolobus solfataricus. Molecular Cell. 2003;11:275–
531 82.

532 35. Hirakawa H, Nagamune T. Molecular assembly of P450 with ferredoxin and
533 ferredoxin reductase by fusion to PCNA. ChemBioChem. 2010;11:1517–20.

534 36. Hirakawa H, Kakitani A, Nagamune T. Introduction of selective intersubunit disulfide
535 bonds into self-assembly protein scaffold to enhance an artificial multienzyme complex's
536 activity. Biotechnology and Bioengineering. 2013;110:1858–64.

537 37. Suzuki R, Hirakawa H, Nagamune T. Electron donation to an archaeal cytochrome
538 P450 is enhanced by PCNA-mediated selective complex formation with foreign redox
539 proteins. Biotechnology Journal. 2014;9:1573–81. doi:10.1002/biot.201400007.

540 38. Hirakawa H, Kamiya N, Tanaka T, Nagamune T. Intramolecular electron transfer in
541 a cytochrome P450cam system with a site-specific branched structure. Protein
542 Engineering Design and Selection. 2007;20:453–9. doi:10.1093/protein/gzm045.

543 39. Haga T, Hirakawa H, Nagamune T. Fine tuning of spatial arrangement of enzymes
544 in a PCNA-mediated multienzyme complex using a rigid poly-L-proline linker. PloS one.
545 2013;8:e75114. doi:10.1371/journal.pone.0075114.

546 40. Tan CY, Hirakawa H, Nagamune T. Supramolecular protein assembly supports
547 immobilization of a cytochrome P450 monooxygenase system as water-insoluble gel.
548 Scientific Reports. 2015;5:8648. doi:10.1038/srep08648.

549 41. Aoki M, Ishimori K, Fukada H, Takahashi K, Morishima I. Isothermal titration
550 calorimetric studies on the associations of putidaredoxin to NADH-putidaredoxin
551 reductase and P450cam. Biochimica et Biophysica Acta (BBA) - Protein Structure and
552 Molecular Enzymology. 1998;1384:180–8. doi:10.1016/S0167-4838(98)00017-X.

553 42. Johnson EOD, Wong L-L. Partial fusion of a cytochrome P450 system by carboxy-
554 terminal attachment of putidaredoxin reductase to P450cam (CYP101A1). Catal Sci
555 Technol. 2016;6:7549–60. doi:10.1039/C6CY01042C.

556 43. Milke L, Aschenbrenner J, Marienhagen J, Kallscheuer N. Production of plant-
557 derived polyphenols in microorganisms: current state and perspectives. Applied
558 Microbiology and Biotechnology. 2018;102:1575–85. doi:10.1007/s00253-018-8747-5.

559 44. Hernández-Chávez G, Martinez A, Gosset G. Metabolic engineering strategies for
560 caffeic acid production in *Escherichia coli*. Electronic Journal of Biotechnology.
561 2019;38:19–26. doi:10.1016/J.EJBT.2018.12.004.

562 45. Santos CNS, Koffas M, Stephanopoulos G. Optimization of a heterologous pathway
563 for the production of flavonoids from glucose. Metabolic Engineering. 2011;13:392–400.
564 doi:10.1016/J.YMBEN.2011.02.002.

565 46. Wu J, Zhou T, Du G, Zhou J, Chen J. Modular Optimization of Heterologous
566 Pathways for De Novo Synthesis of (2S)-Naringenin in *Escherichia coli*. PLoS ONE.
567 2014;9:e101492. doi:10.1371/journal.pone.0101492.

568 47. Stahlhut SG, Siedler S, Malla S, Harrison SJ, Maury J, Neves AR, et al. Assembly of
569 a novel biosynthetic pathway for production of the plant flavonoid fisetin in *Escherichia*
570 *coli*. Metabolic Engineering. 2015;31:84–93. doi:10.1016/J.YMBEN.2015.07.002.

571 48. Sibbesen O, De Voss JJ, Montellano PR. Putidaredoxin reductase-putidaredoxin-
572 cytochrome p450cam triple fusion protein. Construction of a self-sufficient *Escherichia*
573 *coli* catalytic system. The Journal of biological chemistry. 1996;271:22462–9.
574 doi:10.1074/jbc.271.37.22462.

575 49. Robin A, Roberts GA, Kisch J, Sabbadin F, Grogan G, Bruce N, et al. Engineering
576 and improvement of the efficiency of a chimeric [P450cam-RhFRed reductase domain]
577 enzyme. Chemical Communications. 2009;:2478. doi:10.1039/b901716j.

578 50. Bakkes PJ, Biemann S, Bokel A, Eickholt M, Girhard M, Urlacher VB. Design and
579 improvement of artificial redox modules by molecular fusion of flavodoxin and flavodoxin
580 reductase from *Escherichia coli*. Scientific Reports. 2015;5 July:12158.
581 doi:10.1038/srep12158.

582 51. Bakkes PJ, Riehm JL, Sagadin T, Rühlmann A, Schubert P, Biemann S, et al.
583 Engineering of versatile redox partner fusions that support monooxygenase activity of
584 functionally diverse cytochrome P450s. Scientific Reports. 2017;7:9570.
585 doi:10.1038/s41598-017-10075-w.

586 52. Bell SG, Tan ABH, Johnson EOD, Wong L-L, Guengerich FP, Isin EM, et al.
587 Selective oxidative demethylation of veratric acid to vanillic acid by CYP199A4 from
588 *Rhodopseudomonas palustris* HaA2. Mol BioSyst. 2009;6:206–14.
589 doi:10.1039/B913487E.

590 53. Chao RR, De Voss JJ, Bell SG. The efficient and selective catalytic oxidation of
591 para-substituted cinnamic acid derivatives by the cytochrome P450 monooxygenase,
592 CYP199A4. RSC Adv. 2016;6:55286–97. doi:10.1039/C6RA11025H.

593 54. Rodriguez A, Kildegaard KR, Li M, Borodina I, Nielsen J. Establishment of a yeast
594 platform strain for production of p-coumaric acid through metabolic engineering of
595 aromatic amino acid biosynthesis. Metabolic Engineering. 2015;31:181–8.
596 doi:10.1016/J.YMBEN.2015.08.003.

597 55. Rodriguez A, Strucko T, Stahlhut SG, Kristensen M, Svenssen DK, Forster J, et al.
598 Metabolic engineering of yeast for fermentative production of flavonoids. Bioresource
599 Technology. 2017;245:1645–54. doi:10.1016/j.biortech.2017.06.043.

600 56. Juminaga D, Baidoo EEK, Redding-Johanson AM, Batth TS, Burd H,
601 Mukhopadhyay A, et al. Modular engineering of L-tyrosine production in *Escherichia*
602 *coli*. Applied and Environmental Microbiology. 2012;78:89–98.

603 57. Nielsen DR, Yoon S-H, Yuan CJ, Prather KLJ. Metabolic engineering of acetoin and
604 meso-2, 3-butanediol biosynthesis in *E. coli*. Biotechnology journal. 2010;5:274–84.
605 doi:10.1002/biot.200900279.

606 58. Inoue H, Nojima H, Okayama H. High efficiency transformation of *Escherichia coli*
607 with plasmids. Gene. 1990;96:23–8. doi:10.1016/0378-1119(90)90336-P.

608 # Tables

609 Table 1: List of plasmids used in caffeic acid production strains.

Plasmid name	source
IR54 pKVS45::PdR-Pux operon	[18]
IR64 pCDFduet::_6His-CYP199A2 F185L NΔ7	[18]
c22 pRSFduet::6His-RgTAL	This study
c25 pCDFduet::_PCNA3-CYP199A2 F185L NΔ7	This study
c28 pETduet::6His-PCNA2-Pux_PCNA1-PdR (opt)	This study
c50 pETduet::6His-Pux_PdR (opt)	This study
c62 pETduet::6His-Pux_PuR	This study
c63 pETduet::6His-PCNA2-Pux_PCNA1-PuR	This study
c71 pRSFduet::6His-FjTAL	This study
c72 pRSFduet::6His-SeSam8	This study
c84 pCDFduet::6His-Pux_6His-CYP199A2F185L NΔ7	This study
c86 pETduet::6His-Pdx_PdR (opt)	This study
c88 pETduet::6His-PCNA2-Pdx_PCNA1-PdR(opt)	This study
c96 pCDFduet::_PCNA1-GGS-CYP199A2 F185L NΔ7	This study
c97 pETduet::6His-PCNA2-Pux_PCNA3-(GGGS)2-PdR (opt)	This study
c98 pETduet::6His-PCNA2-Pux_PCNA3-(GGGS)2-PuR	This study
c106 pETduet::6His-PCNA2-Pdx_PCNA3-GGS-PdR (opt)	This study

610 Table 2: List of *E. coli* MG1655(DE3) strains used in fermentation experiments.

identifier	Plasmid name	source
s01	IR64 pCDFduet::_6His-CYP199A2 F185L NΔ7 IR54 pKVS45::PdR-Pux operon c22 pRSFduet::6His-RgTAL	This study
s02	IR64 pCDFduet::_6His-CYP199A2 F185L NΔ7 IR54 pKVS45::PdR-Pux operon c71 pRSFduet::6His-FjTAL	This study
s03	IR64 pCDFduet::_6His-CYP199A2 F185L NΔ7 IR54 pKVS45::PdR-Pux operon c72 pRSFduet::6His-SeSam8	This study
s04	IR64 pCDFduet::_6His-CYP199A2 F185L NΔ7 c50 pETduet::6His-Pux_PdR (opt)	This study
s05	IR64 pCDFduet::_6His-CYP199A2 F185L NΔ7 c62 pETduet::6His-Pux_PuR	This study
s06	IR64 pCDFduet::_6His-CYP199A2 F185L NΔ7 c86 pETduet::6His-Pdx_PdR (opt)	This study
s07	c25 pCDFduet::_PCNA3-CYP199A2 F185L NΔ7 c28 pETduet::6His-PCNA2-Pux_PCNA1-PdR (opt)	This study
s08	c25 pCDFduet::_PCNA3-CYP199A2 F185L NΔ7 c63 pETduet::6His-PCNA2-Pux_PCNA1-PuR	This study
s09	c25 pCDFduet::_PCNA3-CYP199A2 F185L NΔ7 c88 pETduet::6His-PCNA2-Pdx_PCNA1-PdR (opt)	This study
s10	c96 pCDFduet::_PCNA1-GGS-CYP199A2 F185L NΔ7 c97 pETduet::6His-PCNA2-Pux_PCNA3-(GGGS)2-PdR (opt)	This study
s11	c96 pCDFduet::_PCNA1-GGS-CYP199A2 F185L NΔ7 c98 pETduet::6His-PCNA2-Pux_PCNA3-(GGGS)2-PuR	This study
s12	c96 pCDFduet::_PCNA1-GGS-CYP199A2 F185L NΔ7 c106 pETduet::6His-PCNA2-Pdx_PCNA3-GGS-PdR (opt)	This study
s13	IR64 pCDFduet::_CYP199A2 F185L NΔ7 c50 pETduet::6His-Pux_PdR (opt) c22 pRSFduet::6His-RgTAL	This study
s14	c25 pCDFduet::_PCNA3-CYP199A2 F185L NΔ7 c28 pETduet::6His-PCNA2-Pux_PCNA1-PdR (opt) c71 pRSFduet::6His-FjTAL	This study
s15	IR64 pCDFduet::_CYP199A2 F185L NΔ7 c62 pETduet::6His-Pux_PuR c71 pRSFduet::6His-FjTAL	This study
s16	c25 pCDFduet::_PCNA3-CYP199A2 F185L NΔ7 c63 pETduet::6His-PCNA2-Pux_PCNA1-PuR c71 pRSFduet::6His-FjTAL	This study

s17	c96 pCDFduet::_PCNA1-GGS-CYP199A2 F185L NΔ7 c106 pETduet::6His-PCNA2-Pdx_PCNA3-GGS-PdR (opt) c71 pRSFduet::6His-FjTAL	This study
s18	c84 pCDFduet::6His-Pux_6His-CYP199A2F185L NΔ7 c62 pETduet::6His-Pux_PuR c71 pRSFduet::6His-FjTAL	This study

Figure captions

Figure 1: Aromatic amino acid anabolism and recombinant caffeic acid pathway with L-tyrosine as a branchpoint, and TAL and CYP199A2 F185L N□7 catalyzing the two pathway steps.

Figure 2: Titers of *p*-coumaric acid and caffeic acid from glucose without (A) and with (B) L-Tyr supplementation (stacked histograms, error bars= standard deviation of biological replicates, n≥3).

Figure 3: The choice of redox partners and tethering strategies for redox partners leads to higher caffeic acid titers from *p*-coumaric acid (panels A-C) and from glucose (panel D). A-C, caffeic acid titers from 3 mM *p*-coumaric acid 72 h p. i.: untethered/free redox partners (A), tether design I analogous to PUPPET [35] (B), tether design II (C). Stacked histograms of *p*-coumaric and caffeic acid titers after 72 h of fermentation for select strains expressing the two-step pathway (D). (Error bars= standard deviation of biological replicates, n≥3; Pictograms of tether designs: P450=Cytochrome P450 enzyme, Fdx=ferredoxin (Pux or Pdx), FdR=ferredoxin reductase (PuR or PdR)).

Figure 4: Duplication of the *pux* gene copy number further increases caffeic acid titers. Stacked histograms of *p*-coumaric and caffeic acid titers after 72 h of fermentation with glucose as the only carbon source for select strains expressing the two-step pathway (A). Titers plotted over time of a 96 h fermentation of s18 (B). (Error bars= standard deviation of biological replicates, n≥3.)

Figures

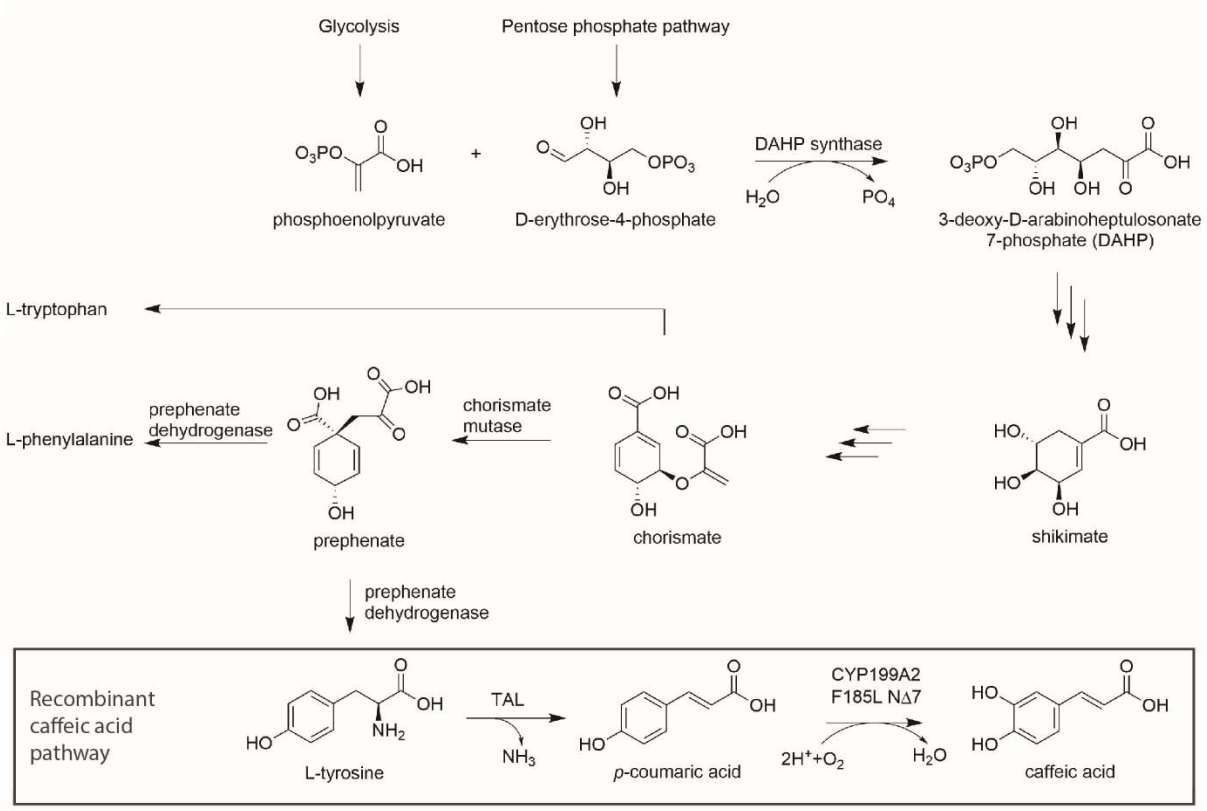

Figure 1

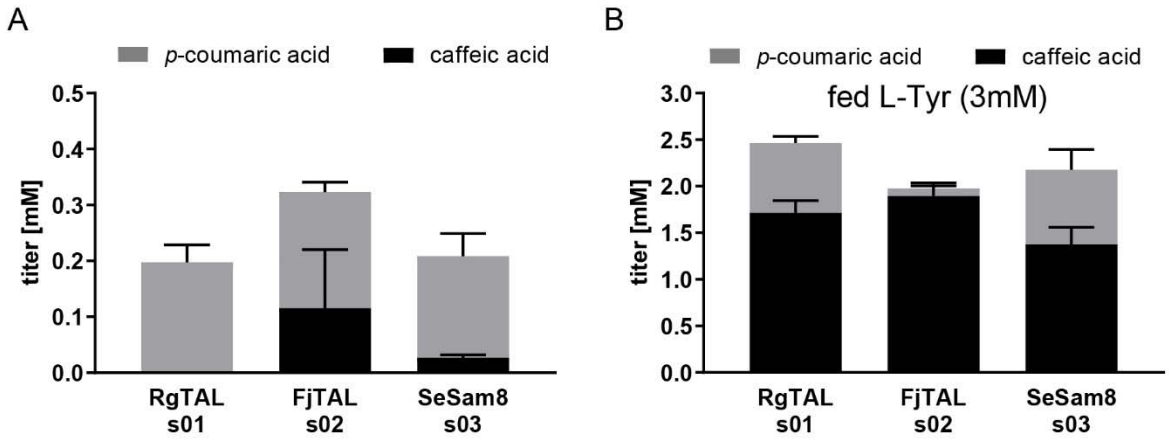

637

638 Figure 2

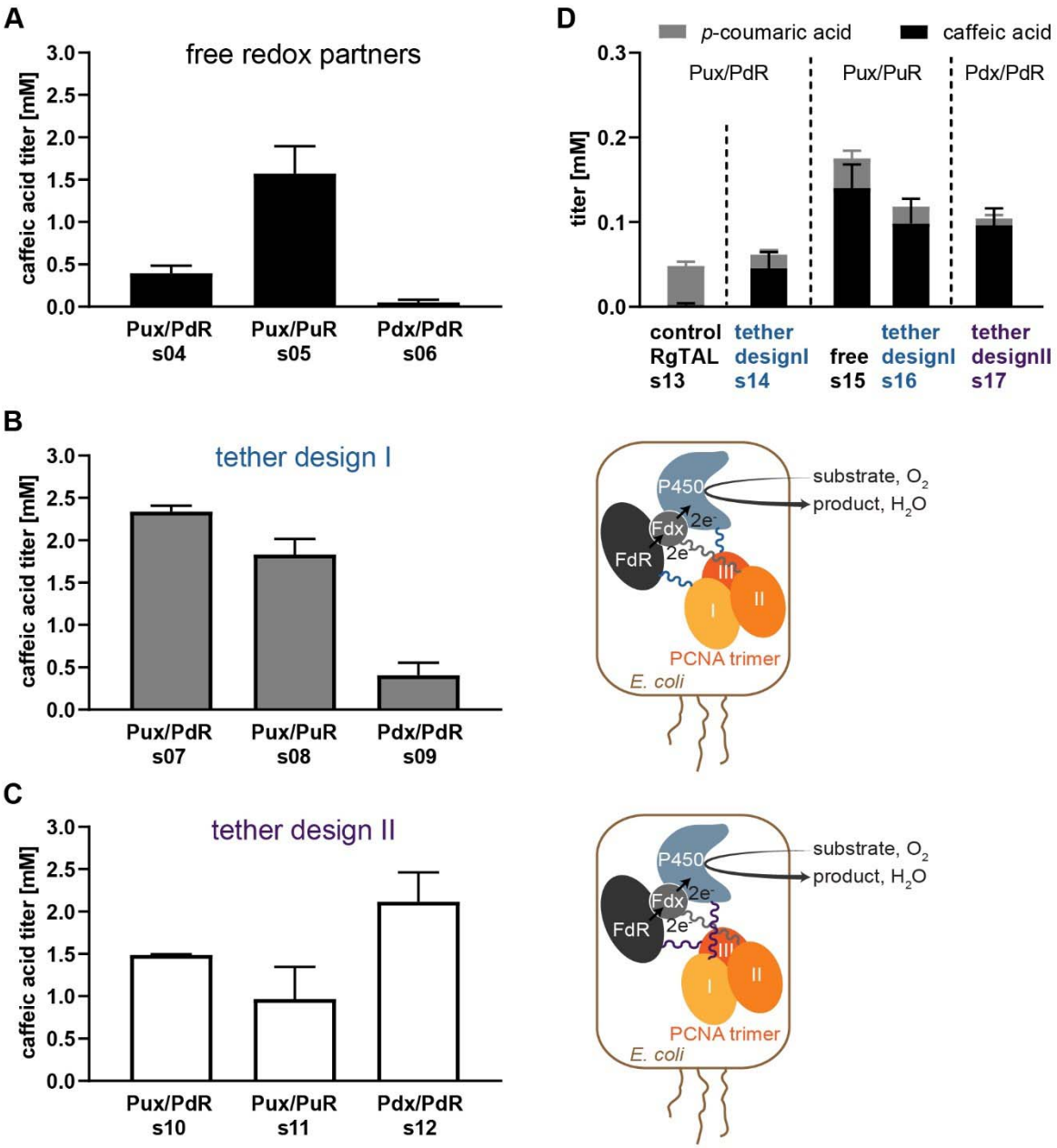

639

640 Figure 3

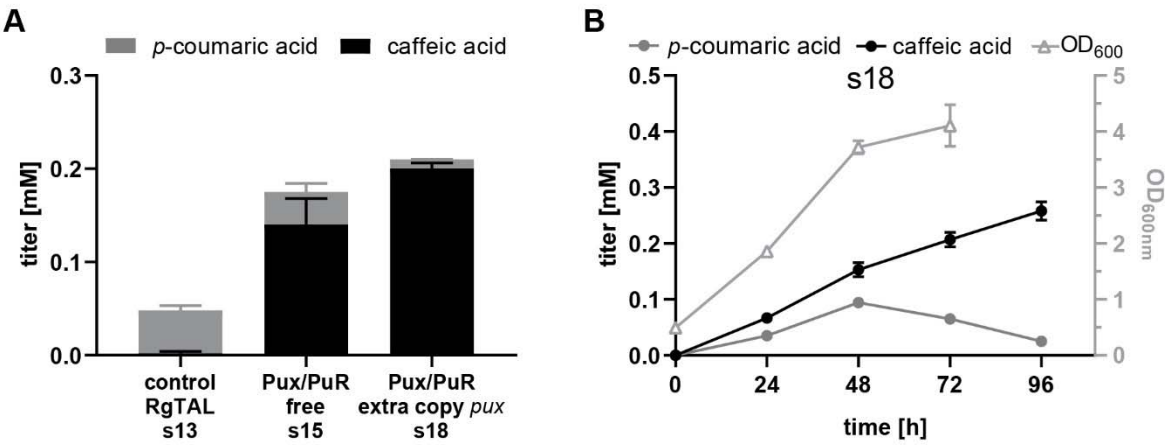

641

642 Figure 4